167 *USE OF MID-LEVEL MODEL DATA AND VAD WINDS TO IMPROVE WSR-88D VELOCITY DEALIASING*

Autumn Losey[1,2*], W. David Zittel[2], and Zhongqi Jing[1,2]
[1]Centuria Corporation, Norman, Oklahoma
[2]NEXRAD Radar Operations Center, Norman, Oklahoma

1. INTRODUCTION

The fielding of the National Weather Surveillance Radar 1988 Doppler radars (WSR-88Ds) in the early 1990's allowed operational forecasters to see the inbound and outbound components of radial winds in a wide variety of weather conditions for the first time. To obtain velocity data, the WSR-88D uses a pulse repetition frequency (PRF) that balances the maximum unambiguous range with the maximum non-aliased velocities. From hardware design considerations, these values can be specified by the equations

$$V_{max} = \frac{\pm PRF\,\lambda}{4} \quad (1)$$

and

$$V_{max}R_{max} = \frac{c\lambda}{8} \quad (2)$$

where V_{max} is the maximum non-aliased velocity, R_{max} is the maximum unambiguous range, c is the speed of light, and λ is the radar's wavelength (Rinehart 2010). For the WSR-88D's ~10 cm wavelength, the practical paired limits of V_{max} and R_{max} are ~32.0 ms^{-1} / ~117 km and ~21.5 ms^{-1} / ~175 km. The corresponding PRFs are ~1282 s^{-1} and ~857 s^{-1}, respectively.

To be operationally useful, range unfolding and velocity dealiasing are required to extend the usable data range to 300 km at elevation angles < 2.0° and to 230 km at or above 2.0°, and usable velocities to at least 60 ms^{-1} at all elevation angles (0.5° - 19.5°). Obtaining good velocity estimates is vital to the mission of the National Weather Service.

Recently, at least three WSR-88D sites observed regions of incorrectly dealiased velocity data as new radar echo moved into their areas of coverage, necessitating a major change to the default dealiasing scheme, the Two-Dimensional Velocity Dealiasing Algorithm (2DVDA). This paper gives a brief overview of the velocity dealiasing algorithms used by the WSR-88D with emphasis on the 2DVDA, describes the conditions leading to a rare but significant failure mode, describes a solution that uses model data with Velocity Azimuth Display (VAD) estimates of the free atmosphere wind (FAW), and finally, shows the application of the solution to various cases.

**Corresponding author address:* Autumn Losey, NEXRAD Radar Operations Center 1313 Halley Circle, Norman, OK 73069; email: autumn.d.losey@noaa.gov.

2. BACKGROUND

Currently, there are three velocity dealiasing algorithms available in the WSR-88D: the legacy Velocity Dealiasing Algorithm (VDA; Eilts and Smith 1990), the Multi-PRF Velocity Dealiasing Algorithm (MPDA; Conway et al 1997; Zittel 2008), and the newest (now default), the 2DVDA (Jing and Wiener 1993; Witt et al 2009; Zittel and Jing 2012). Each algorithm, to some extent, uses an external source of wind information to help with dealiasing. Historically, the WSR-88D's Radar Product Generator (RPG), using its own Velocity Azimuth Display (VAD) algorithm, created a VAD Wind Profile (VWP) product and populated a current wind profile that could be used by the legacy VDA. This created a feedback loop where the quality of the wind profile depended on the quality of velocity dealiasing, which depended on good estimates in the wind profile. In 2007, the RPG began ingesting the Rapid Update Cycle (RUC) model data on an hourly basis from the National Weather Service's Advanced Weather Interactive Processing System (AWIPS). In 2012, the Rapid Refresh (RAP) model data replaced the RUC. The RPG repopulates the current wind profile with model wind data. The current wind profile copy of this table is updated each volume scan by RPG's Enhanced VWP (EVWP) algorithm (Chrisman and Smith 2009). The RPG maintains a separate "clean" copy of the model data, which is updated with each model update. These wind profiles are available for use by the velocity dealiasing algorithms.

2.1 Legacy VDA

The legacy VDA is simplest in concept and requires the least computer resources. It relies primarily on radial continuity and velocity averages of nearby bins in the current and a previously dealiased “good” radial. After the first radial is dealiased, its results are saved for comparison to the next new radial if the radial is deemed “good.” If the dealiasing in the new current radial is deemed unreliable due to unresolved shear, its results are put in the output velocity field but will not be saved for comparison to the next radial. The last “good” radial is retained instead and a count of “bad” radials is incremented. When a threshold count of “bad” radials is reached, the legacy VDA initiates a fresh start to dealiasing. Upon the start of an elevation, or if it encounters problems finding good nearby bins to use in dealiasing, the VDA will use data from the current wind profile. In regions of strong shear, the legacy VDA occasionally has large, wedge-shaped regions of incorrectly dealiased velocities.

2.2 MPDA

The MPDA acquires velocity data from up to three sequential scans at the same elevation with each scan using a different PRF for elevation angles up to and including 4.5°. At higher elevations, Doppler scanning matches that of other volume coverage patterns (VCPs). It uses the redundancy provided by multiple velocity estimates at the same point in space to provide reliable estimates of dealiased velocity data. Because of range folding and the natural evolution of weather echo, some points in space may have only two velocity estimates or just one. Where there is only one estimate, the MPDA will use the environmental wind profile to assist with velocity dealiasing. The MPDA is best suited for large, slowly moving systems such as hurricanes and large winter systems, and for mountainous terrain where azimuthal continuity is negatively impacted. Because of its reliance on multiple scans at the same elevation and time constraints, the number of unique elevations sampled is limited to nine and it requires its own unique VCP (VCP 121). Therefore, the use of the MPDA is minimal.

2.3 2DVDA

The 2DVDA is the most complex of the three dealiasing techniques. The 2DVDA dealiases connected two-dimensional regions within an elevation scan by minimizing all detected velocity discontinuities. It calculates the difference between a gate and the neighboring gates, puts paired gates into a smoothness function, and applies a least squares method to find suitable velocity values that minimize the smoothness function. To realize the full potential of the two-dimensional approach, the 2DVDA must be applied to a full elevation scan. This is done in two phases. In phase one, the full field is used to generate an environmental wind table. In order to conserve computer CPU and memory resources, the 2DVDA sub-samples large, complex fields. This is done by subsampling regions within the velocity field azimuthally and radially and computing a median velocity value for the center of each grid. In phase two, the 2DVDA partitions the elevation scan and then dealiases smaller features such as mesocyclones and tornado vortex signatures. Finally, the internally generated environmental wind table is used to place small, isolated regions in the correct Nyquist co-interval.

In the interest of increasing 2DVDA’s robustness, a number of improvements have been added since its initial discussion in Jing and Wiener 1993. This section will discuss these enhancements in order to give context to the status of 2DVDA when the failures were observed. Most enhancements mentioned in Zittel and Jing 2012 are still in use: weighting velocity differences to reduce the contribution of noisy data to the optimization setting, separating regions connected by a narrow “bridge” of noisy data, and the temporary removal of sidelobe-contaminated data. Others have been removed once it was determined that they either harmed or did not contribute to the dealiasing solution, such as using spectrum width to help weight velocity differences. Since then, other enhancements have been added. These include: identifying and dealiasing region boundaries to predetermine the full region’s aliased state, the addition of a gust front detection function to improve the quality of the background wind field, the addition of a simple storm base estimation algorithm to correct the data altitude in case of high vertical shear, using simple linear interpolation to improve the calculation of the vertical wind analysis portion of the 2DVDA’s internal VAD, a radial extrapolation method that provides better background wind for dealiasing remote hurricane cells, and finally, saving a history of environmental and storm features to restore after a task restart.

The 2DVDA relies almost completely on its own internally developed VAD wind profiles and a three-dimensional background wind field. It uses model wind data upon initial task startup or if two volume scans have elapsed without any usable

background wind field being available. This limited use of model data led to the failure mode described in the next section.

3. 2DVDA FAILURE MODE

Between August 2015 and July 2016, the Radar Operations Center's Hotline received reports of significant velocity dealiasing errors from three radar sites: Sioux Falls, SD (KFSD) on 7 August, 2015, Tallahassee, FL (KTLH) on 17 January 2016, and Hastings, NE (KUEX) on 29 June 2016. The situations at these sites shared several features. In terms of weather, all cases began during quiescent periods with echo return from clutter and/or biota limited to the surface boundary layer near the radar. Velocity data near the radars were very light or nearly uniform in direction with little veering. Soundings from nearby or collocated sites show that all had strong upper level systems with uniform winds from a westerly direction, with speeds increasing from the surface to a maximum between 30 and 40 kft and then decreasing above the peak. Figures 1a, 1c, and 1e show the sounding direction and speed profiles paired with velocity images in Figures 1b, 1d, and 1f for each of the three cases. Although one could argue that radar velocities at far range are a logical extrapolation of the near-radar velocities, it is clear they should have the same direction as the sounding winds.

As previously mentioned, the WSR-88D has a range of PRFs from which to choose for obtaining velocity data. This PRF diversity allows the radar to maximize detection of important features such as mesocyclone and tornado signatures. If velocity data are dealiased incorrectly, then a change in the PRF results in a distinct shift in the distribution of the incorrectly dealiased velocity data. Figures 2a-d show a pair of images from KFSD for two back-to-back volume scans at 2312 UTC and 2316 UTC, first incorrectly dealiased as outbound velocities (Figures 2a and 2b), and then correctly dealiased as inbound velocities (Figures 2c and 2d). Note the shift in the distribution of the incorrectly dealiased outbound velocities (change from mostly yellow to red and pinks) and no shift in the distribution of the correctly dealiased (green) inbound velocities.

A more subtle effect is that the magnitude of incorrectly dealiased velocities decreases with increasing range, which is equivalent to increasing height. From the sounding wind speed profiles, it is clear that correctly dealiased velocities should be increasing with height. Combining vertical profiles of dealiased velocity data with model data provides the solution described in the next section. This failure mode has been present since the original fielding of the 2DVDA, evidenced by replaying the same cases with the original code and observing the same errors.

4. SOLUTION – MODEL DATA AND FREE ATMOSPHERIC WIND IN 2DVDA

The solution to the failure mode is to allow 2DVDA to use model data to assist with velocity dealiasing at long range. For the remainder of the paper, the terms "model data" and "external wind" are interchangeable. The new code, henceforth known as the External Wind enhancement, represents the first real effort to use model data in 2DVDA on a consistent basis. The most significant addition in terms of code is the computation of the Free Atmospheric Wind (FAW).

FAW is based on the assumption that the wind direction between 3 and 9 km in altitude is nearly uniform in the radar coverage area. When sufficient radar data exist for any given elevation angle within this 3-9 km atmospheric depth, 2DVDA dealiases the data twice – once with a positive Nyquist co-interval and once with a negative Nyquist co-interval. It then performs VAD analysis on the data to produce two potential FAW values. (Note that this VAD analysis is independent of the existing analysis that creates 2DVDA's internal VAD.) Echo coverage must span 150° in azimuth at elevations lower than 2°, and must span 75° in azimuth at elevations of 2° or higher.

Each FAW estimate has an associated wind speed, wind direction, root mean square (RMS), and 0^{th}-order Fourier coefficient. To determine which FAW estimate to use, these values are compared as follows. When the wind directions are less than one degree apart, the estimate with the smaller 0^{th}-order Fourier coefficient is chosen and given high confidence. Otherwise, when the wind directions are more than one degree apart, the estimate with a substantially smaller RMS will be chosen and given high confidence. If one estimate's RMS is small enough to be chosen over the other, but is not small enough to be given high confidence, this estimate has low confidence and will not be used immediately. Instead, it is stored until the end of the volume scan. If a high-confidence FAW cannot be calculated, these low-confidence estimates can be used to check for vertical consistency. Vertical consistency compares previous estimates from different elevations in the same volume scan; if these estimates have minor differences in both speed

and direction, vertical consistency is established. The difference in average speed must be either less than 10 ms^{-1}, or less than one-third of the FAW estimate speed. The difference in direction must be no more than 30°. In this instance, the newest low-confidence estimate is averaged with the speeds and directions of the previous estimates and becomes the new FAW. If the estimates have large differences in speed or direction, vertical consistency is not established and no FAW is computed for that elevation scan.

FAW is used to verify the VAD and model data – again, only if sufficient data both exists in the correct altitude and is close enough to the radar. Therefore, many volumes may pass before VAD and model data are verified, which has potential data quality consequences depending on the quality of model data. This is discussed in a later section. Verification of VAD and model data involves comparing the successfully computed FAW with VAD and model data in the correct altitude range. When their speeds and directions are close in value to the FAW, the VAD and model data are verified as good.

In the event that VAD does not fall within a threshold speed and direction based on the FAW, the existing VAD is discarded and the FAW becomes the basis for a new set of VAD records. This can have negative impacts on the dealiasing solution if the FAW itself is faulty; however, some checks exist for the FAW. For instance, the azimuthal data span requirement (mentioned earlier) prevents FAWs from being generated before sufficient return exists to give a complete picture of the mid-level winds. The exclusion of FAW estimates for supplemental low-level elevation scans prevents overweighting the winds for those elevations. Finally, a vertical wind speed check will discard FAW estimates that exceed a threshold negative slope, which contradicts the assumptions made in the code about the actual free atmosphere. While the negative slope could be true, it is more likely to be false, and accepting it would cause dealiasing errors. If the negative slope is true and the FAW estimate is rejected, then the model data will be retained.

In addition to the FAW, the External Wind enhancement allows 2DVDA to reference model data more frequently. Even so, model data is still treated with caution. When storms are near the radar or when the internal VAD has been verified by FAW, model data is not used. Also, once model data is verified as either good or bad by FAW, it is no longer used since FAW verifies VAD at the same time.

5. TESTING

5.1 Test Cases

To test the software changes to 2DVDA, 16 total cases were examined. Besides the three cases that exposed the problem, 13 additional cases were selected to ensure that no deterioration in dealiasing quality ensued from the new code and to test the criteria for FAW robustness. All cases and their attendant weather are listed in Table 1.

The KFSD, KTLH, and KUEX cases were the instigating cases that exposed the failure mode. All three featured storms moving in from the west from a distance. One case had similar weather coming from the east and was included to ensure 2DVDA made no assumptions about the direction of the atmospheric flow. Two wintertime cases were chosen to see how the new code handled low Nyquist velocities of approximately 12 ms^{-1}. Two cases with data from Hurricane Irene were selected because the large-scale circulation requires special handling when generating VAD-based wind profiles. Two tornadic cases were included to ensure there were no adverse effects on small-scale circulations aloft. A third tornadic case was included to check that the new code correctly handled data with sectorized use of different PRFs within an elevation scan. One case used the Supplemental Adaptive Intravolume Low-level Scan (SAILS; Daniel et al. 2014) during severe weather and was included to ensure the new code handled extra low-level elevations properly. Two cases were mostly clear air; one featured enhanced return from biota, while the other showed smoke bloom from a grass fire. One case transitioned from minimal echo insufficient to generate an internal VAD to showers without strong winds aloft. Finally, a case from the WSR-88D testbed used Staggered PRT data (Torres et al. 2009). Operational VCPs that include the SPRT waveform may be fielded in the near future on WSR-88Ds.

5.2 Model Data / External Wind Simulation

Although RAP model data is available to the field via AWIPS, it was not saved as part of the Level II data stream prior to the latest software release (Build 17), and was not available to non-operational, offline systems during testing. To create a viable approximation to model data, the ROC developed an offline tool to enter sounding data into the model profile accessed by 2DVDA. To facilitate testing, soundings close in time and

location to the test radar site were chosen. Table 2 lists the sounding used for each case and summarizes the ways in which the soundings were altered for different aspects of testing.

5.2 Playback Runs

Each of the sixteen cases was run at least three times. For the first run, 2DVDA used model data to provide a realistic image of what field users originally saw. The second run used 2DVDA with selected heights from a representative sounding as proxy model data to provide the solution as field users would see it. Finally, the third run was repeated using 2DVDA with selected heights from different non-representative soundings as proxy model data to provide stress testing for the new code.

5.3 Scoring

Each run was scored based on the degree and quantity of differences between velocity solutions, regardless of the dealiasing quality. This was to limit the scope of the analysis to the correction of the relevant velocity dealiasing failures, as well as to ensure the new code did not deteriorate the 2DVDA's overall performance. The instigating cases were additionally scored based only on the size of the dealiasing errors.

A trinary categorical scoring scheme was used for both scoring methods. No or isolated errors or differences were scored as a zero. Small, mostly contiguous patches of errors or differences were scored as a one. Errors or differences encompassing large wedges or over half the solution were scored as a two. Figure 3 shows an example of each category.

5.4 FAW / External Wind Status Output

In order to study FAW generation and specific times when model data was used, status messages from log output generated by 2DVDA were collected with each run. Figure 4 shows an example of log output. The 2DVDA log output captures FAW generation and reports the wind speed and direction of the FAW estimate, along with the time at which the FAW was generated. The 2DVDA also monitors the status of model data, which it reports in the log file. Every elevation, the model data may be reported as unavailable, newly received, available, verified bad, or verified good. In order to categorize the log messages for plotting, each relevant external wind message was assigned an arbitrary number from negative one to two, as shown in Table 3. Multiple messages may come up in one elevation.

6. RESULTS

6.1 Overall Results

As mentioned earlier, testing involved running each data case at least three times. The results of these runs were compared for differences in velocity solutions and the composite results are discussed below.

6.1.1 No Model Data vs Good Model Data

Of the sixteen cases considered, ten showed no difference between these comparisons. The majority of these cases did not use model data at all due to the presence of storms near the radar, although they did generate FAW. For those that used model data, the lack of differences implies that adding good model data had no impact on dealiasing results when sufficient echo coverage created a reliable internal VAD. Of the six that showed differences, KFSD, KTLH, and KUEX showed the greatest change. As these were the original problem cases, this was expected – the changes are due to the correction of the dealiasing errors. In addition, the east-moving storm case and the two wintertime cases showed slight improvements.

6.1.2 Good Model Data vs Non-Representative Model Data

The comparison of good to non-representative model data served to determine how well the External Wind enhancement filters out the bad model data. Five out of sixteen cases showed no differences between good and bad model data solutions – again, due to the presence of storms near the radar. Three cases with differences were, of course, KFSD, KTLH, and KUEX. The non-representative model data degraded the dealiasing solution until the FAW could verify the model data as bad. Of the remaining cases, four showed degraded performance in only the first volume; this was a consequence of the limitations of non-operational playback. Non-operational playback will clear out 2DVDA's internal VAD upon startup, whereas in the field, VAD history would have been available. 2DVDA would then reject the bad model data. The east-moving storm case and one of the clear air cases showed negative differences because insufficient coverage hindered consistent FAW computation. The two wintertime cases were difficult to dealias even with

FAW because of the presence of fronts and the low Nyquist velocity of ~12 m s^{-1}. This testing did illustrate the External Wind enhancement's sensitivity to bad model data. Further non-representative runs were executed to test how sensitive the code is to differing degrees of non-representativeness.

6.2 Dealiasing Errors – Instigating Cases

For the three instigating cases (KFSD, KTLH, and KUEX), raw dealiasing errors were tabulated using the same trinary categorization as the data run comparisons. Table 4 summarizes these errors, grouping the run using original data without the External Wind enhancement, the run using the External Wind enhancement with no model data (FAW only), and the run using the External Wind enhancement with good model data (good model data and FAW). Interestingly, the number of errors decreases in each grouping, implying that the FAW by itself improved the dealiasing results. A closer look at the code controlling the FAW and its relationship to 2DVDA's phase 1 (summarized in section 2.3) explains this finding. The FAW doesn't require model data to activate – in the absence of model data, 2DVDA will still check the latest FAW estimate against the internal VAD. As earlier described, the FAW will replace a non-representative internal VAD, which in most cases is enough to correct the velocity dealiasing errors. KTLH shows greater improvement than the other cases because the weather moved in quickly enough for FAWs to be generated earlier.

6.3 Use of Non-Representative Model Data

Non-representative model data were generated by modifying the proxy sounding data in one or multiple ways. The direction was modified using an offset between 30° and 180°, while velocity was modified by either increasing the values by a factor of 1.5 or 2.0, or by adding an offset of 50 kts. The final column in Table 2 shows the combination of speed and direction adjustments made to the good model data. If the original velocity data are well below the Nyquist velocity, the quality of the dealiased data will not be affected by non-representative model data speed. Also, if there is sufficient return to generate FAWs, non-representative wind profiles are flagged as bad. This is important when there are new returns at altitudes above the maximum height of 2DVDA's internal VAD.

Non-representative wind profiles can negatively affect the quality of velocity dealiasing when there is insufficient echo to generate FAWs. The KFSD case at 2207 UTC on 7 August 2015 (Figures 5a-d) shows how dealiasing is affected. Figure 5a shows the dealiasing results with no model data. Figure 5b shows correct dealiasing results using good proxy model data. Figure 5c shows that having a wind direction diametrically opposed to the good direction produces the same error as having no profile. Finally, Figure 5d shows errors introduced when the wind speed is increased to 1.5 times the original value at all levels while maintaining the original directions. In Figure 5a, some small regions with correct inbound velocities have incorrect outbound velocities in Figure 5c. In Figure 5d, part of the image shows the correct inbound velocities and part of the image shows inbound velocities increased by the Nyquist co-interval, which appear as bright pink – the maximum possible inbound velocity.

The FAW checks the quality of the external wind for each volume scan and each elevation angle and flags it as either good or bad. In a control case from KDDC from 16 May 16 2015 (not shown) where the echo coverage always ensured generation of an FAW, deviations in the sounding direction were tested at 180°, 90°, 60°, 50°, and 30°. At all deviations but the 30° deviation, the external wind was flagged as bad. Even within the 30° directional deviation, several elevation cuts were flagged as bad.

6.4 Case Study – Tallahassee, FL (KTLH)

One of the instigating cases occurred January 17, 2016. From about 0200 to 0300 UTC, the radar was using VCP 32 and afterwards used VCP 212. This case featured widespread precipitation approaching the radar from the southwest, with light winds near the surface and much stronger winds aloft (above the FAW 3-9km range). See Figure 1c for the sounding used as proxy model data. Figure 1d shows an example of the dealiasing failures reported by the field. The dealiasing errors KTLH originally showed were corrected with the new code and good proxy model data. Errors were introduced using non-representative proxy model data.

Figure 6 shows a time series of FAW estimates and their elevation angles (blue lines). Individual blue dots show the starting time of each elevation scan. Downward-sloping lines show increasing elevation and steep, upward-sloping lines show the start of a new volume. The short volumes before 0311 UTC are in VCP 32, while all those after that time are VCP 212. The volumes in VCP 212 use SAILS. The site was also running

Automated Volume Scan Evaluation and Termination (AVSET), which terminates VCPs at elevation angles below 19.5° if the echo is below area and strength thresholds. As the weather approaches the radar, AVSET terminates the VCP at higher elevations (Chrisman 2009). The FAW speeds (red dots) are initially over 90 kts (46 ms^{-1}) but decrease to about 70 kts (36 ms^{-1}) after 0330 UTC. The FAW directions (green dots) are initially estimated to be about 220° azimuth, shifting to about 200° azimuth at 0345 UTC. Note the relatively close clustering of the FAW speed and direction estimates. This suggests that the quality control measures within the new code are successfully filtering unrealistic estimates.

Studying KTLH's external wind messages from the log file also proved instructive. Figure 7 illustrates exactly how the External Wind enhancement affects the data. This plot shows the external wind log messages on the left y-axis and the count of large differences by volume on the right y-axis. The x-axis is the data time in UTC. The legend shows the number associated with each log message. The first feature to note on this plot is the external wind messages. All model data starts as "unavailable," indicated by the pair of markings on the '0' line. This is another artifact of non-operational playback. Immediately afterward, both good model data (purple circles) and bad model data (yellow squares) are "available," which means 2DVDA is using them to help build a dealiasing solution. Then, at 0300 UTC, the good model data is verified as good and the bad model data is verified as bad for the rest of the playback. Now, note the solid lines that comprise the bottom half of the plot. These represent the count of large differences by volume. The red, green, and orange lines all represent comparisons to good or bad model data. Because of this, the differences fall to zero when external wind is verified since model data is no longer used. The blue line, however, is a comparison between original data played back without the External Wind enhancement and data played back with the External Wind enhancement, but without model data. The differences increase when the verification messages begin, as this coincides with the generation of FAW. Once FAW is generated, the dealiasing failures are corrected. The slight steps in the blue line are due to gradually increasing numbers of elevations within the volumes from changing VCPs and from AVSET. The other noteworthy feature of Figure 7 comes from comparing the green line, which is good model data compared to model data with non-representative direction, and the orange line, which is good model data compared to model data with non-representative speed. Because both are compared to good model data, differences represent instances where the bad model data has caused dealiasing errors. Aside from the first volume or two, the green line consistently represents a greater amount of errors than the orange line, implying that the External Wind enhancement is more sensitive to non-representative directions than speeds.

7. CONCLUSIONS

The changes to the 2DVDA code to reference model data and to generate a midlevel (3 to 9 km) estimate of the free atmospheric wind (FAW) successfully remove the dealiasing errors observed in the three instigating cases KFSD, KTLH, and KUEX while having no adverse effects on cases not showing that type of dealiasing error. In the absence of model data, the FAW can reduce velocity dealiasing failures. Simulations of non-representative model data demonstrate that dealiasing errors could be introduced via "bad" model data. Therefore, computing an FAW provides a method to minimize effects of errors in the model data.

8. ACKNOWLEDGMENTS

The authors gratefully acknowledge the contribution of Zachary Biggs to the data analysis. The authors also thank the reviewers within the Applications Branch of the ROC as well as other ROC staff who provided comments and feedback.

9. REFERENCES

Chrisman, J.N., 2009: Automated Volume Scan Evaluation and Termination (AVSET): A simple technique to achieve faster volume scan updates. *34th Conf. on Radar Meteor, Williamsburg, VA Amer. Meteor. Soc., P4.4.* [Available online at https://ams.confex.com/ams/34Radar/techprogram/paper_155324.htm].

Chrisman, J.N. and S.D. Smith, 2009: Enhanced velocity azimuth display wind profile (EVWP) function for the WSR-88D. *34th Conf. on Radar Meteor, Williamsburg, VA Amer. Meteor. Soc., P4.7.* [Available online at https://ams.confex.com/ams/34Radar/techprogram/paper_155822.htm].

Conway, J.W. K.D. Hondl, and M.D. Eilts, 1997: Minimizing the Doppler Dilemma using a unique redundant scanning strategy and multiple pulse repetition frequency dealiasing algorithm. *Preprints: 28th Conf. on Radar Meteor,* Austin, TX, AMS, 315-316.

Daniel, A. E., J. N. Chrisman, C. A. Ray, S. D. Smith, and M. W. Miller, 2014: New WSR-88D operational techniques: Responding to recent weather events. *Proc. 30th Conf. on Environmental Information Processing Technologies*, Atlanta, GA, Amer. Meteor. Soc., 5.2. [Available online at https://ams.confex.com/ams/94Annual/webprogram/Paper241216.html.]

Eilts, M. D. and S. D. Smith, 1990: Efficient dealiasing of Doppler velocities using local environment constraints. *J. Atmos. Oceanic Technol.*, **7**, 118-128.

Jing, Z. and G. Wiener, 1993: Two-Dimensional Dealiasing of Doppler Velocities. *J. Atmos. Oceanic Technol.*, **10**, 798-808.

Rinehart, R.E., 2010: *Radar for Meteorologists*. 5th ed. Rinehart Publishing, 482 pp.

Torres, S., D. Zittel, and D. Saxion, 2009: Update on development of staggered PRT for the NEXRAD network. Preprints, *25th International Conference on Interactive Information and Processing Systems (IIPS) for Meteorology, Oceanography, and Hydrology*, Phoenix, AZ, P11B.2.

Witt, A., R. A. Brown, and Z. Jing, 2009: Performance of a new velocity dealiasing algorithm for the WSR-88D. *34th Conf. on Radar Meteorology*, Williamsburg, VA, Amer. Meteor. Soc. P4.8. [Available online at http://ams.confex.com/ams/34Radar/techprogram/paper_155951.htm].

Zittel, W. D and Z. Jing, 2012: Comparison of a 2-D velocity dealiasing algorithm to the legacy WSR-88D velocity dealiasing algorithm during Hurricane Irene. *30th Conf. on Hurricanes and Tropical Meteorology,* Jacksonville/Ponte Vedra, FL, AMS, 7C.7.

Zittel, W. D., and Coauthors, 2008: Combined WSR-88D technique to reduce range aliasing using phase coding and multiple Doppler scans. *24th Conf. on Interactive Information and Processing Systems (IIPS) for Meteorology, Oceanography, and Hydrology*, New Orleans, 21-25 January, P2.9.

A.1 TABLES

Site	Date	Time (UTC)	VCP(s)	Type of Weather
KFSD	07 Aug 2015	2100 to 0000	32/212/12	Strong storms moving in from west
KTLH	17 Jan 2017	0200 to 0400	32 / 212	Widespread precip moving in from west
KUEX	20 Jun 2016	0000 to 0228	212/11	Storms moving in from northwest
PGUA	30 Aug 2015	0100 to 0400	21	Scattered showers drifting westward
KDDC	16 May 2015	1100 to 1300	212	Severe storms w/MESO_SAILS
KTLX	20 Jun 2013	1900 to 2100	12	Tornadic Storms
KTLX	31 May 2013	2300 to 0100	212	Tornadic Storms
KDMX	03 Dec 2008	1200 to 1600	31	Winter precip / frontal boundaries
KTLX	26 Jan 2009	2000 to 0000	31	Winter precip / frontal boundaries
KTLX	10 May 2010	2200 to 2300	12/212	Tornadic Storms w/ Sectorized PRFs
KLTX	27 Aug 2011	0300 to 0600	212	Hurricane Irene
KAKQ	27 Aug 2011	2000 to 0000	212	Hurricane Irene
KCBW	26 Jan 2014	0300 to 0445	32 / 31	Clear air case / Storms
KOUN	05 Nov 2015	1800 to 2200	113	Squall line in test VCP 113 MPDA for split cuts, SPRT/2DVDA for batch cuts and CD cuts
KVNX	18 Feb 2016	2000 to 0000	32	Smoke plume
KDDC	07 Sep 2015	1100 to 1400	32	Biological bloom

Table 1: List of cases tested with for the External Wind enhancement

WSR-88D Site	Sounding Site	Date / Time (UTC)	Sounding Profiles Tested
KFSD	KABR	08 Aug 2015 0000	(spd, dir), (spd, dir+180°), (1.5*spd, dir)
KTLH	KTLH	17 Jan 2016 0000	(spd, dir), (spd, dir+180°), (2.0*spd, dir)
KUEX	TOP	29 Jun 2016 0000	(spd, dir), (spd, dir+180°), (1.5*spd, dir)
PGUA	PGAC	30 Aug 2015 0000	(spd, dir), (spd+50, dir+90°)
KDDC	KDDC	16 May 2015 1200	(spd, dir), (spd, dir+180°), (spd, dir-90°)°), (spd, dir-60°)°), (spd, dir-50°)°), (spd, dir-30°)
KTLX	KOUN	20 May 2013 1800	(spd, dir), (spd, dir+180°)
KTLX	KOUN	01 Jun 2013 0000	(spd, dir), (spd+50, dir+90°)
KDMX	KOAX	03 Dec 2008 1200	(spd, dir), (spd, dir+180°)
KTLX	KOUN	26 Jan 2009 1200 27 Jan 2009 0000	(spd, dir), (spd, dir+180°), (spd, dir-30°)
KTLX	KOUN	11 May 2010 0000	(spd, dir), (spd+50, dir+90°)
KLTX	KMHX	27 Aug 2011 0600	(spd, dir), (spd, dir+180°)
KAKQ	WALLOPS	28 Aug 2011 0000	(spd, dir), (spd+50, dir+90°)
KCBW	KCBW	26 Jan 2014 0000	(spd, dir), (spd, dir+180°)
KOUN	KOUN	05 Nov 2015 1800	(spd, dir), (spd, dir+180°)
KVNX	KOUN	19 Feb 2016 0000	(spd, dir), (spd, dir+180°)
KDDC	KDDC	07 Sep 2015 1200	(spd, dir), (spd+50, dir+90°)

Table 2: Sounding sites paired to WSR-88D sites, where spd is speed in knots and dir is direction in degrees for each reported height. The “good” soundings are shown as (spd, dir); non-representative soundings have an offset added to the direction and either an offset or a multiplicative value applied to the speed.

External Wind Message (Good or Bad Data)	Arbitrary Associated Value
External wind verified as good	2
External wind available	1
External wind not available	0
External wind verified as bad	-1

Table 3: External Wind Messages from the veldeal.log file and their assigned values.

	Original Data			FAW Only			Good Model Data & FAW		
	KFSD	KTLH	KUEX	KFSD	KTLH	KUEX	KFSD	KTLH	KUEX
Number of Volumes	28	20	37	28	20	37	28	20	37
No Errors (0's)	61	7	125	127	141	275	237	155	315
Minor Errors (1's)	23	9	16	22	9	9	0	0	1
Large Errors (2's)	153	139	175	88	5	32	0	0	0
Total # Elevation Scans	237	155	316	237	155	316	237	155	316

Table 4: Total Raw Velocity Dealiasing Errors – “Original Data” refers to the data without the External Wind enhancement. “FAW Only” refers to data with the External Wind enhancement with no proxy model data available. “Good Model Data and FAW” refers to data with the External Wind enhancement with representative proxy model data. Note the decrease in errors in each successive grouping.

A.2 FIGURES

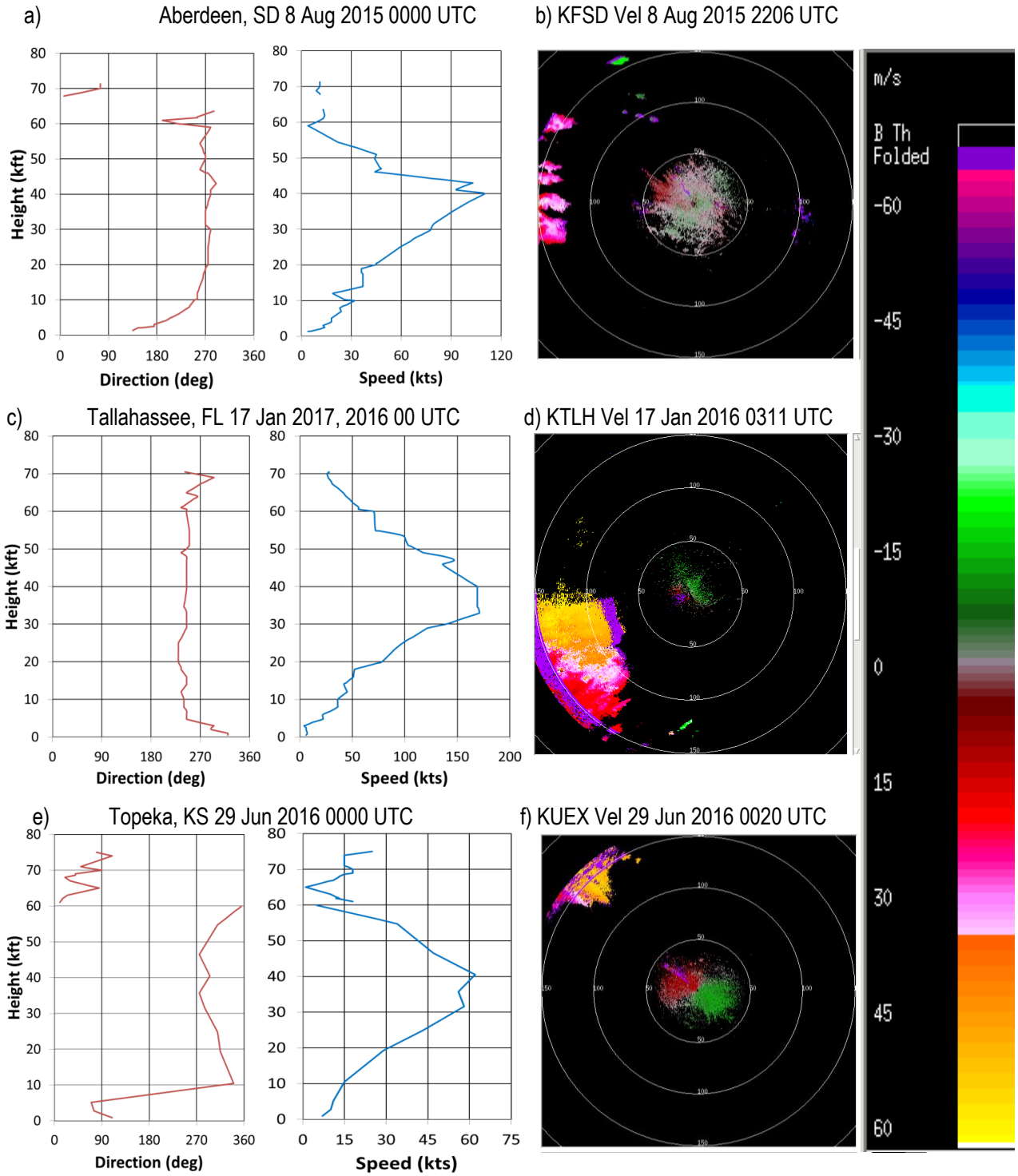

Figure 1: Shows sounding wind direction and speed profiles for sites nearby or collocated with the three WSR-88D sites that showed dealiasing errors. Aberdeen, SD (a) was paired with the Sioux Falls, SD (KFSD) radar (b), Topeka, KS (c) was paired with the Hastings, NE WSR-88D (d), and KTLH (e) and radar (f) are collocated. The radar velocity data in each case are diametrically opposed to the wind profile shown in the sounding.

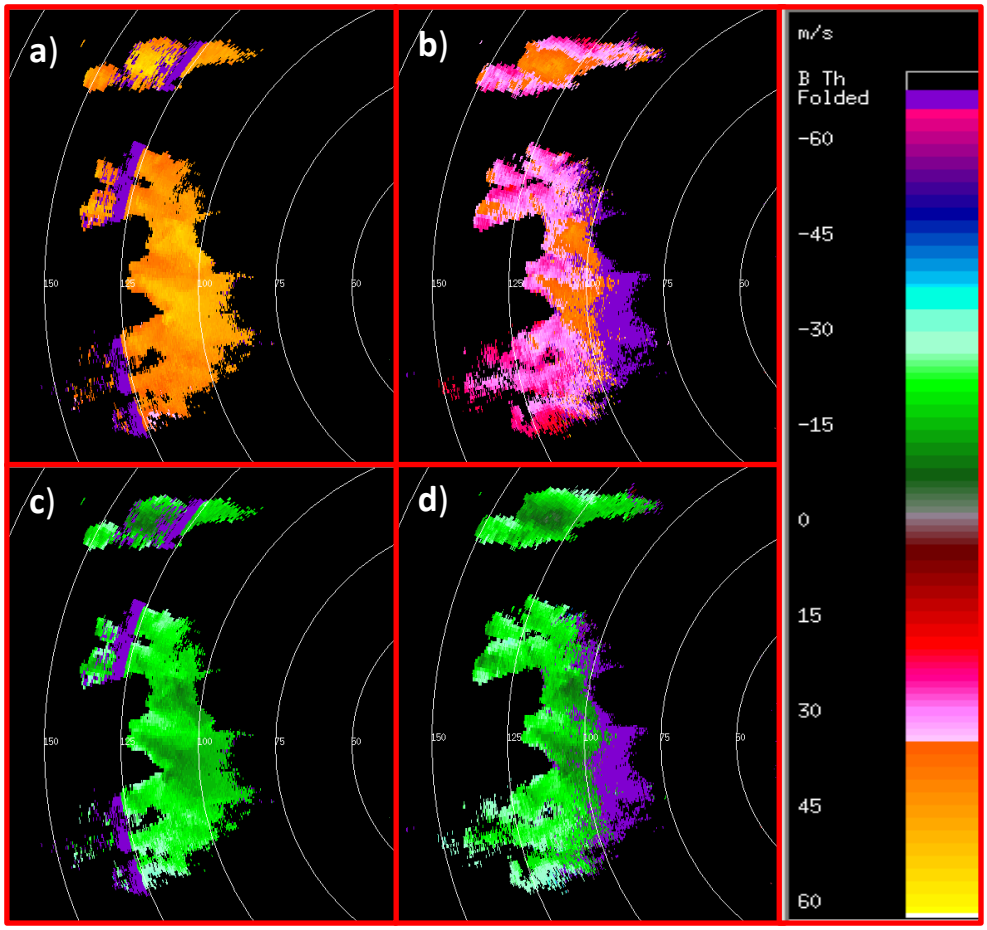

Figure 2: KFSD velocity data 8 August 2015 at 2312 UTC (left panels a and c) and at 2316 UTC (right panels b and d). The top panels are incorrectly dealiased while the bottom two panels are correctly dealiased. Note the change in colors between the top two panels due to the change in PRF indicated by the shift in the range folded (purple) regions. The velocities are shifted from about 45 m s^{-1} to about 30 m s^{-1}. The lower panels show no such shift.

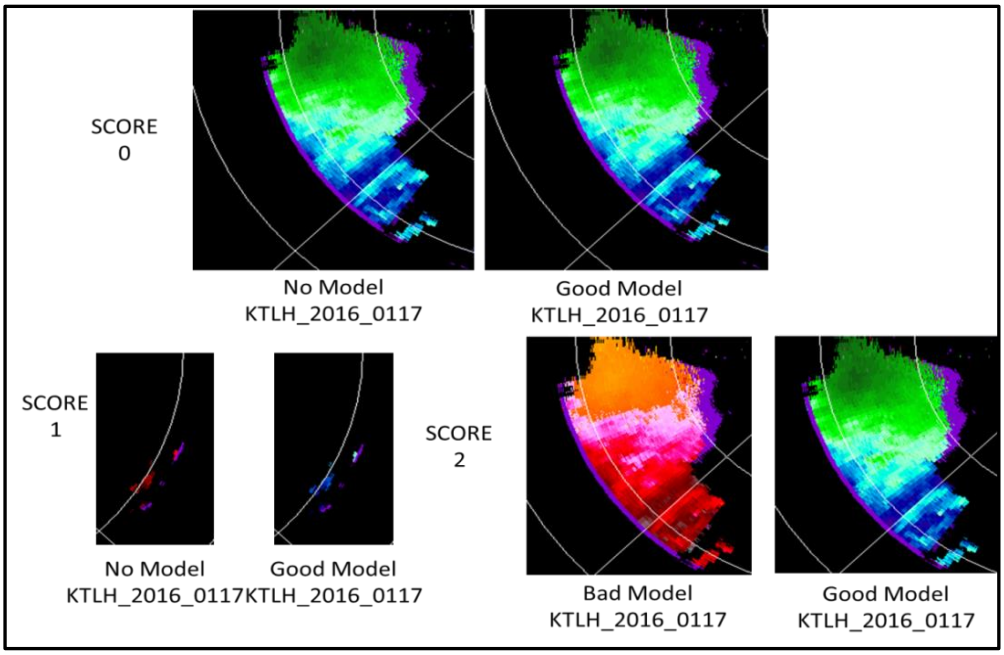

Figure 3: Example of scoring between playback runs. The left images of each pair can represent pure error scoring, while the pair represents a comparison scoring. No or few errors/differences are 0's. Minor patches of errors/differences are 1's. Large (over half the return) errors/differences are 2's.

Example Log Ouput - KTLH

```
13:17:50   veldeal: Use adapt data: VDB_threads 4; VDD_threads 8; max_partition_size 103
13:17:50   veldeal: Start of elevation 0.50 (azi 110.25) 2016_01_17_02_07_58
13:19:05   veldeal: Estim. BW (ele 0.5, st azi 110), nyq 53
13:19:05   veldeal: External wind not available
13:19:05   veldeal: New external wind received - verified to 0

13:20:17   veldeal: Start of elevation 1.50 (azi 119.25) 2016_01_17_02_10_24
13:21:31   veldeal: Estim. BW (ele 1.5, st azi 119), nyq 53
13:21:31   veldeal: External wind available

14:10:08   veldeal: Start of elevation 4.50 (azi 130.49) 2016_01_17_03_01_01
14:11:31   veldeal: Estim. BW (ele 4.5, st azi 130), nyq 57
14:11:31   veldeal: External wind available
14:11:31   veldeal: FAW analysis: Good FAW found spd 101 dir 220
14:11:31   veldeal: VAD wind is set to good by verification
14:11:31   veldeal: External wind is set to good by verification

14:12:41   veldeal: Start of elevation 0.50 (azi 174.82) 2016_01_17_03_03_44
14:13:56   veldeal: Estim. BW (ele 0.5, st azi 175), nyq 57
14:13:57   veldeal: External wind verified as good; VAD verified as good
```

Figure 4: Snippets of the velocity dealiasing task's log output file for the KTLH case with good external winds provided.

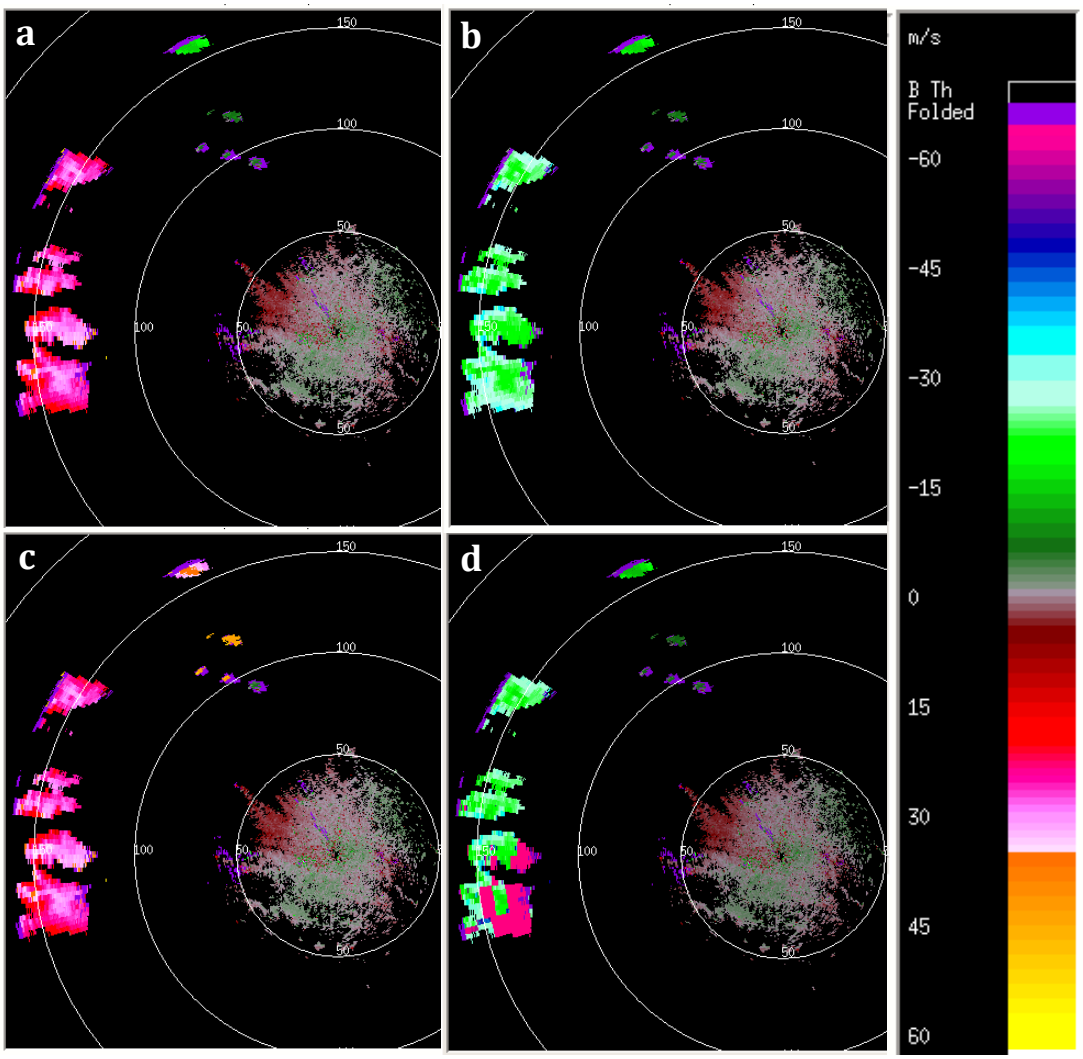

Figure 5: These images show the dealiasing results from Sioux Falls, SD (KFSD) on 7 August 2015 at 2207 UTC for varying external wind profiles. a) Incorrectly dealiased outbound velocity data with no proxy sounding. b) Correctly dealiased inbound velocity data using a good proxy sounding. c) Incorrectly dealiased outbound velocity data with the proxy sounding direction rotated 180°. d) Patches of partially incorrect inbound velocity data with the proxy sounding speed increased by a factor of 1.5. In 5d, the velocity errors are at the maximum possible inbound value of -63.5 m s^{-1} (123 kts).

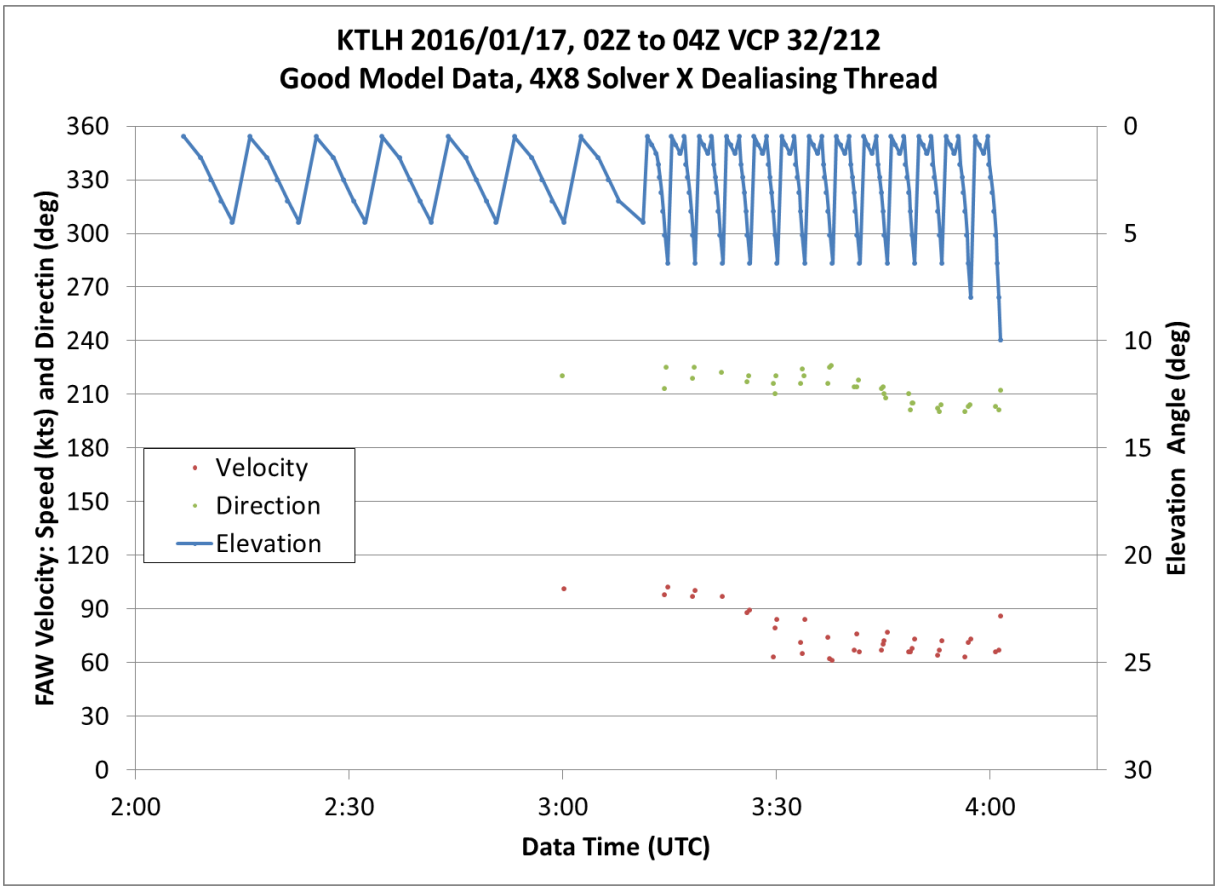

Figure 6: KTLH FAW time series. The left axis is the FAW speed and direction in knots and degrees, respectively. The right axis is the elevation angle in degrees. The odd gap at 0311 UTC is due to the truncation of the last elevation of VCP 32. The way the data time is calculated for the plot cannot account for this.

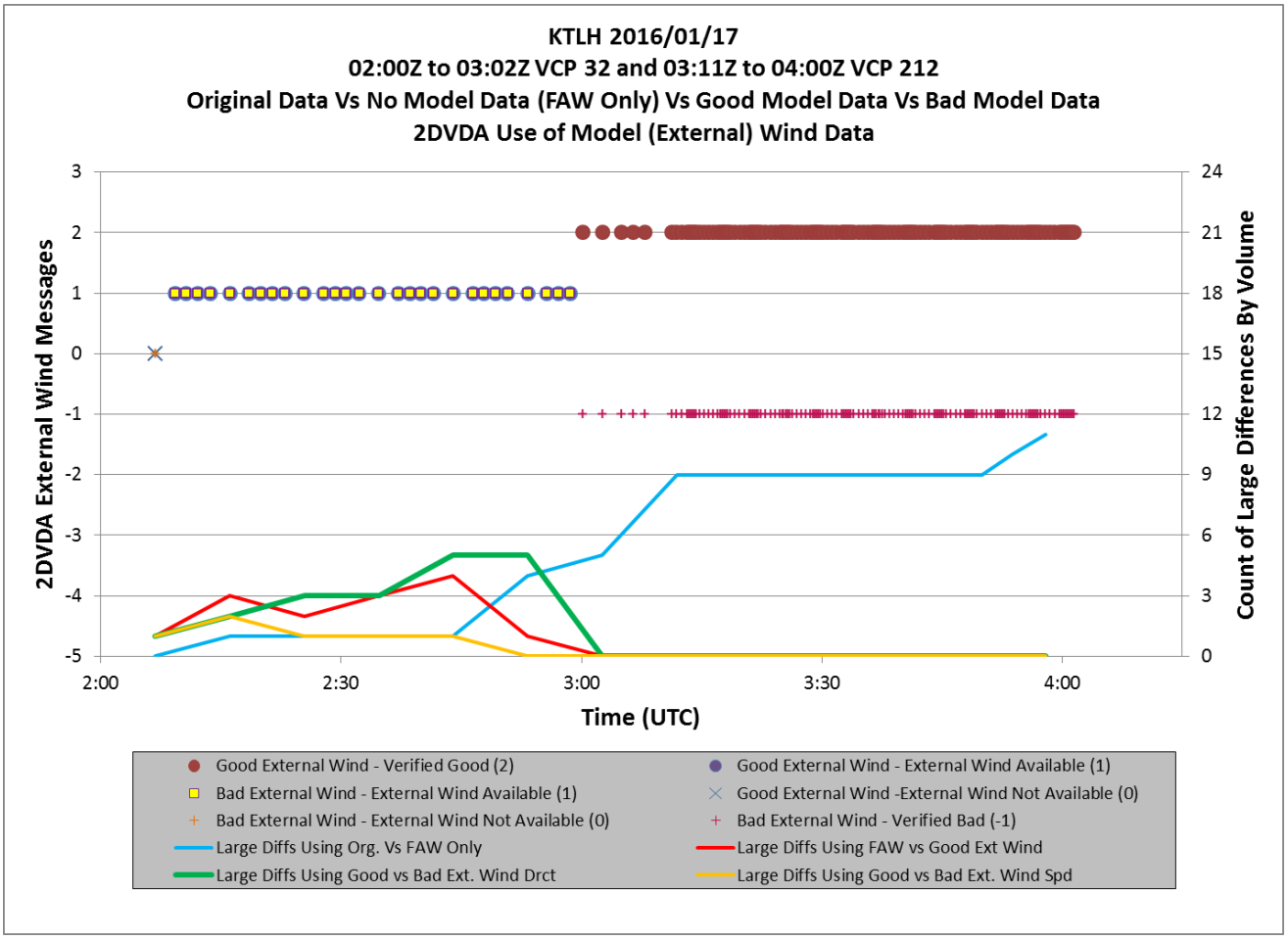

Figure 7: External Wind messages and the count of large differences by volume for each comparison run. Note in the legend that each external wind message has its associated value in parentheses at the right. At the very start of the case, no model data is available. Then, model data is available all the way up until 0300 UTC, when it is verified as good or bad. Since both bad runs of model data (one with bad speed, one with bad direction) had the same messages at the same time, they are shown together for simplicity. The slight discrepancy in time is due to the difference in time scale between the FAW estimates and the average computations. The FAW time is the exact time of the estimate; the averages are taken over a volume.